3

Volume 15
September 2014
ISSN 1464-4177

Structural Concrete

Journal of the *fib*

- Building bridges using the balanced lift method
- Concrete integral abutment bridges with RC piles
- Consistent practical design of concrete structures
- Evaluation of design shear resistance of RC slabs
- Experiments for punching behaviour of RC footings
- Behaviour of round CFST columns
- Effect of welding heat on composite columns
- Minimum flexural rebar amount in rectangular and T-beams
- Influence of time-dependent effects on crack spacing in RC beams
- Stochastic fracture-mechanical parameters for performance-based design
- Reliability-based post-fire assessment framework for concrete slabs
- Effect of bond degradation due to corrosion – a review
- Review of potential lunar base building materials

Ernst & Sohn
A Wiley Brand

fib
CEB-FIP

The cover picture shows the Egg-Graben Bridge which was a winning structure in the 2014 competition for the *fib* Awards for Outstanding Concrete Structures. In the words of the jury "The jury highly appreciated the consistent application of durability philosophy. The bridge deck is intended to have a long service life with very low maintenance costs because the bridge deck is constructed exclusively with encapsulated post-tensioned reinforcement and watertight anchorages. No other reinforcement is used. Therefore, the electrolytic corrosion in the deck is ruled out. In this way waterproofing and pavement were also saved. The concrete itself is meant to resist both physical and environmental loads. The bridge also fulfils high aesthetic expectations." More information can be found in this issue on pp. 281–291 (photo: *Pez Hejduk*).

Structural Concrete

Vol. 15 / 3

September 2014
ISSN 1464-4177 (print)
ISSN 1751-7648 (online)

Wilhelm Ernst & Sohn
Verlag für Architektur und technische
Wissenschaften GmbH & Co. KG
www.ernst-und-sohn.de

fédération internationale
du béton
International Federation
for Structural Concrete
www.fib-international.org

Journal of the *fib*

Peer reviewed journal
Since 2009, *Structural Concrete* is indexed in Thomson Reuter's Web of Knowledge (ISI Web of Science).

Impact Factor 2013: 0.857

Wiley Online Library

www.wileyonlinelibrary.com, the portal for Structural Concrete online subscriptions

Technical Paper

Deok Hee Won
Woo Sun Park
Jin-Hak Yi
Sang-Hun Han
Taek Hee Han*

DOI: 10.1002/suco.201300060

Effect of welding heat on precast steel composite hollow columns

Steel composite hollow columns have been studied in order to ease their construction. Welding or bolting are mostly used for connecting the steel tubes of precast steel composite hollow columns. However, welding generally results in temperatures of about 20000 °C in the welding zone and 1300 °C around the welding zone. Thus, the strength of the concrete in regions close to a welding zone is reduced. In this paper, the effects of arc welding and electro-slag welding – two widely used methods for connecting the column modules of steel composite hollow columns – on the temperature change in the welding zone are studied by performing heat transfer analysis. The changes in the strength of the concrete are investigated for each welding method. The rate of decrease in concrete strength due to electro-slag welding was greater than that due to arc welding. In addition, an effective method using ceramic fibres is suggested for preventing strength reduction in concrete due to welding heat.

Keywords: welding, heat, column, precast, concrete

1 Introduction

Interest surrounding precast columns is increasing in the construction industry because of their high constructional efficiency. Precast columns, consisting of individual modules fabricated in a factory, are assembled on the construction site. There are several ways of assembling these columns, e.g. column-bent cap, column segment-segment joints and column-foundation. These connections must exhibit good performance to prevent the global failure of a column. Furthermore, it is important to select the type of connection and column cross-section to ensure safe construction. Steel composite hollow members have good ductility and strength compared with hollow RC columns. This type of member was developed in the late 1980s [1] for use as a substructure in bridges and as a column in buildings. Fig. 1a shows a steel composite hollow member; double steel tubes are arranged concentrically and the space between them filled with concrete. The concrete experiences a triaxially confining state because it is restrained by the double steel tubes that exert passive lateral pressure on the concrete in the radial direction. Therefore, the strength of steel composite hollow members is generally 10–30 % greater than the sum of the strengths of its individual components. Furthermore, these members exhibit good seismic performance because of the composite effect of steel-concrete interactions [2].

A precast steel composite hollow column has three types of connection: a) connection between column segment modules, b) connection between bent cap and column, and c) connection between column and foundation. The connection between column segments was suggested in [3], and is shown in Fig. 1b. A precast steel composite hollow column is composed of internal and external tubes plus concrete. Connections must be proposed for the concrete and the tubes. These connections must resist bending moments and shear forces under lateral loads. As only the tubes resist the bending moments, all tubes must be bonded perfectly [4]. The method for connecting steel tubes is welding, which is a high-probability, high-performance method of connecting steel. Stiffeners in the internal and external columns are connected by fillet welding after the steel tubes are joined by groove welding, as shown in Fig. 1b. For welding the internal tube to a stiffener, an auto welding machine or manual welding can be used because this column system is generally used in large piers and wind turbine towers. This method of connection requires a certain welding space in the hollow section. Its diameter needs to be at least 1.5 m. This connection is suggested large section that diameter of hollow section has over 1.5 m.

Fig. 1c shows cracks in the concrete in the welding zone of a precast steel composite column [4]. This specimen was selected after using the connecting method shown in Fig. 1b. The internal and external tubes of precast steel composite hollow column modules were connected by groove welding, whereas the internal and external stiffeners on the internal and external tubes were connected by fillet welding. The structural behaviour of precast steel composite hollow columns was investigated using the quasi-static test method, an experimental method for applying constant axial force and repetitive lateral force to the top of a column. According to the results of this experiment, concrete cracking mostly occurred in the welding zone, and the colour of the concrete in the welding zone changed to lampblack. Welding heat directly (or indirectly) influences precast column behaviour. Welding heat leads to temperatures of about 20000 °C in the weld zone and about 1300 °C in regions around the

* Corresponding author: taekheehan@kiost.ac

Submitted for review: 31 July 2013
Revised: 12 December 2013
Accepted for publication: 2 January 2014

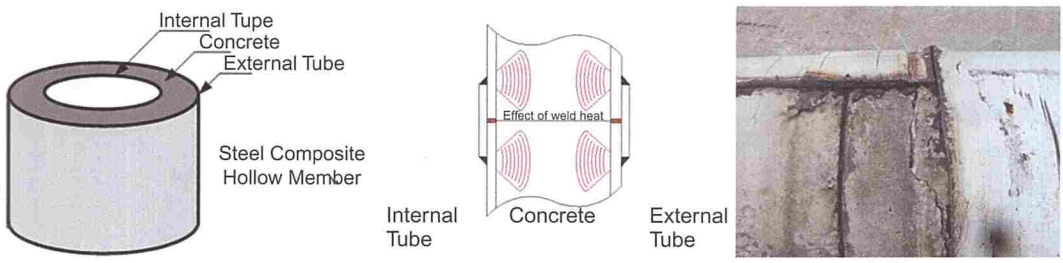

Fig. 1. Section and module connections for steel composite hollow columns: a) section through column, b) connection method for modules, and c) cracks in concrete

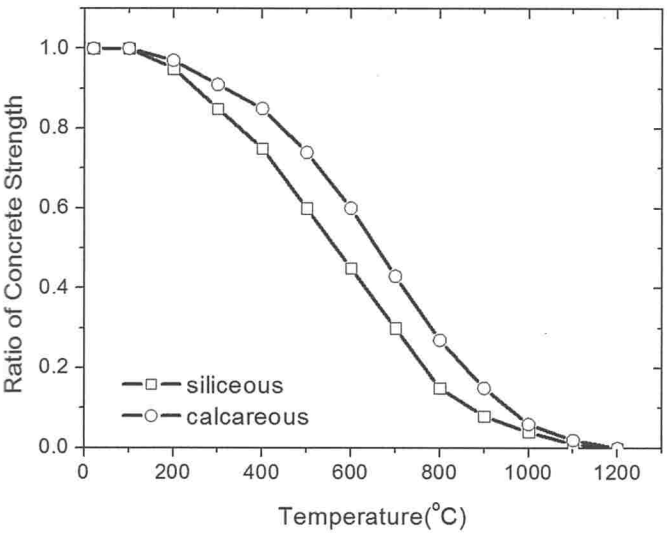

Fig. 2. Variation in concrete strength due to temperature rise [5]

weld zone. Furthermore, welding heat is transferred to the concrete from the welding zone. The strength of the concrete near the welding zone is reduced due to the massive increase in temperature. The change in concrete strength with rise in temperature, shown in Fig. 2, is based on Eurocode 2 [5].

Fig. 2 shows the variations in concrete strength with change in temperature, as outlined in Eurocode 2 [2]. They are divided into siliceous and calcareous concrete based on their mineral content because the properties of concrete change depending on their constituent materials. Using the above curves, the strength change induced by welding heat can be estimated. It is obvious that a partial change in concrete strength may influence the behaviour of an entire column system [6, 7]. This paper investigates the effect of welding heat on the changes in the structural behaviour and load-carrying capacity of precast steel composite hollow columns. By comparing the effects of arc welding and electro-slag welding on concrete strength, we propose an effective method for preventing the reduction in concrete strength due to welding heat.

2 Heat transfer analysis

This study investigates the conduction of welding heat in concrete members based on the results of [8]. Table 1 lists the material properties of steel and concrete which should be considered during heat transfer analysis [9].

For heat transfer analysis, steel and concrete are modelled with 4-node linear elements called DC2D4. Thermal loads are applied to the tube surfaces as described in a previous experimental study [8]. Eq. (1) describes the standard time-temperature curve [10]:

$$T = 345 \cdot Log_{10}(8t + 1) \quad (1)$$

where T denotes the heating temperature (°C) and t denotes time (min).

Table 1. Properties of steel and concrete with temperature change [9]

Steel				Concrete			
Temp. °C	Specific heat J/kg · °C	Thermal conductivity J/kg · mm · °C	Density mg/mm³	Temp. °C	Specific heat J/kg · °C	Thermal conductivity J/kg · mm · °C	Density mg/mm³
0.00	449.91	197.97	7.85	0.00	1260.12	8.46	2.35
93.58	484.64	185.89	7.82	93.58	1314.12	6.44	2.33
105.04	488.88	184.41	7.81	105.04	5256.5	6.19	2.33
114.59	492.42	183.18	7.81	114.59	3036.52	5.98	2.32
197.35	523.11	172.51	7.78	197.35	954.09	5.84	2.3
398.55	597.74	146.55	7.7	398.55	983.25	5.51	2.26
700.57	872.51	107.59	7.59	700.57	1207.07	5.00	2.18
750.39	1046.05	101.16	7.57	750.39	1232.11	4.92	2.17
827.59	687.49	91.25	7.54	827.59	1270.92	4.79	2.15
850.03	583.28	92.23	7.53	850.03	1282.22	4.75	2.15
1200.00	674.87	108.18	7.40	1200.00	1458.14	4.17	2.07

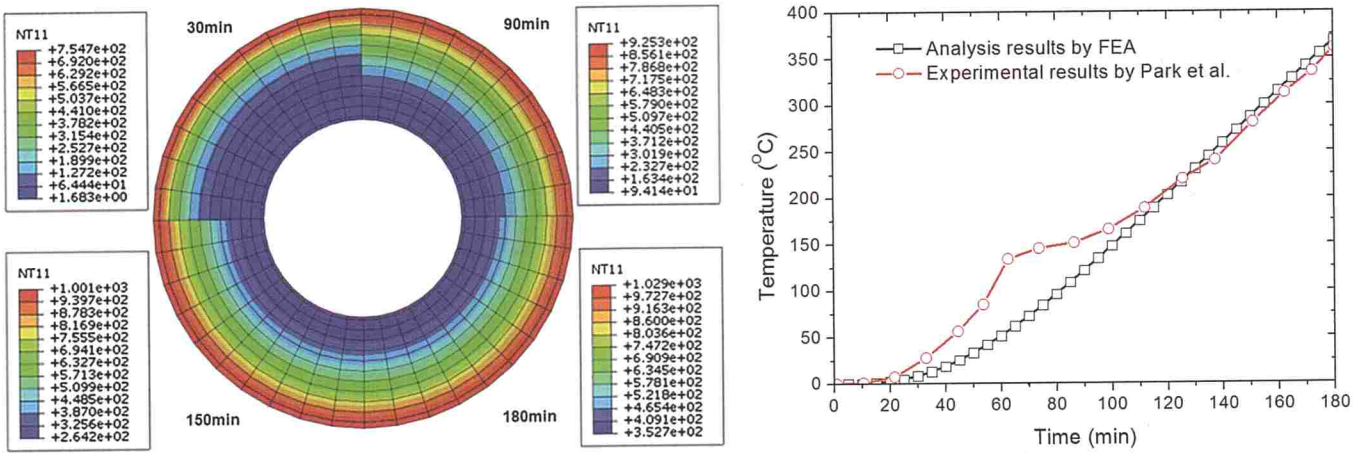

Fig. 3. Results of heat transfer analysis in steel composite hollow column: a) heat transfer analysis, and b) temperature at D/4 of column

These dimensions are used for verifying the analysis method. *Park* et al. used the following dimensions for a steel composite hollow column [8]: diameter of column = 406.4 mm, thicknesses of external and internal tubes = 9 and 7.1 mm respectively, and diameter of hollow core = 150 mm. A heat transfer analysis was performed using the material properties and dimensions of the aforementioned steel composite hollow column.

Fig. 3a shows the temperature distributions in our analysis at 30–60 min intervals. Thermal load is conducted towards the hollow face from the surface of the external tube. Fig. 3b shows a comparison of the temperature changes at D/4 of the diameter as obtained in the heat transfer analysis performed in this study. The figures indicate that as time passes, the temperature at D/4 of the column diameter increases gradually, and the tendency for a temperature rise obtained through heat transfer analysis is similar to that obtained experimentally [8]. The comparison results show that the analysis method is reasonable and that it can be used for investigating the conduction of welding heat through a precast steel composite hollow column.

3 Changes in concrete strength with type of welding heat

3.1 Welding heat and application

Electric arcs are the most common heat sources driving welding heat transfers. The temperature distribution around the heat source cannot be changed because of the steady-state transfer. The heat generated by a heat source can be calculated using Eq. (2):

$$HE = \frac{E \times I}{S} \times 60 \tag{2}$$

where:
HE calories per unit length (J)
E arc voltage (V)
I welding current (A)
S transfer distance per minute (mm/min)

Eq. (2) is used to calculate the heat generated during arc welding and for comparing various welding methods. Time-temperature curves for arc and electro-slag welding are proposed in [11].

The Time-temperature curves of the two welding methods have several differences, such as rates of temperature increase and decrease and peak temperatures, as shown in Fig. 4. The Time-temperature curve obtained by arc welding fluctuates rapidly. By contrast, in electro-slag welding the temperature increase and decrease is relatively gradual. The thermal load induced by welding heat is applied using the Time-temperature curves shown in Fig. 4. During heat transfer analysis, point loads are applied to the surfaces of the internal and external tubes. The dimensions of the precast steel composite hollow column used for the heat transfer analysis were as follows: column diameter = 2500 mm, hollow ratio = 0.7, external tube thickness = 39.5 mm, internal tube thickness = 33.18 mm.

Welding is performed simultaneously on the faces of the inner and outer tubes of the steel composite hollow column. Fig. 5a shows the temperature distribution during arc welding, as obtained by heat transfer analysis. The legends of each part represent the exterior of external tube (E1), interior of external tube (E2) and concrete

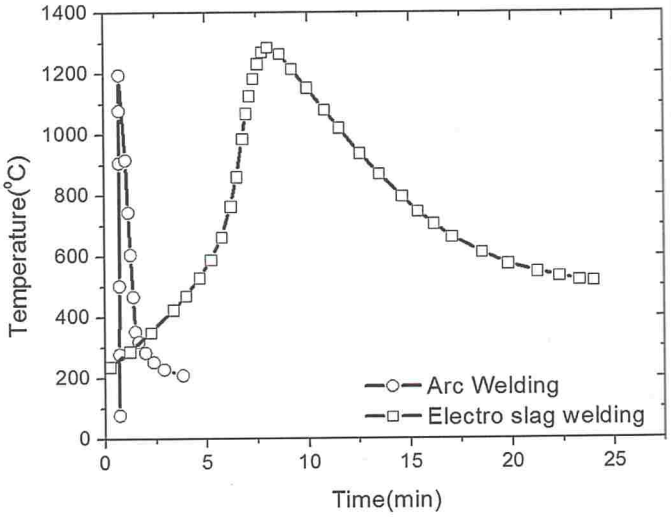

Fig. 4. Time-temperature curves for various welding methods

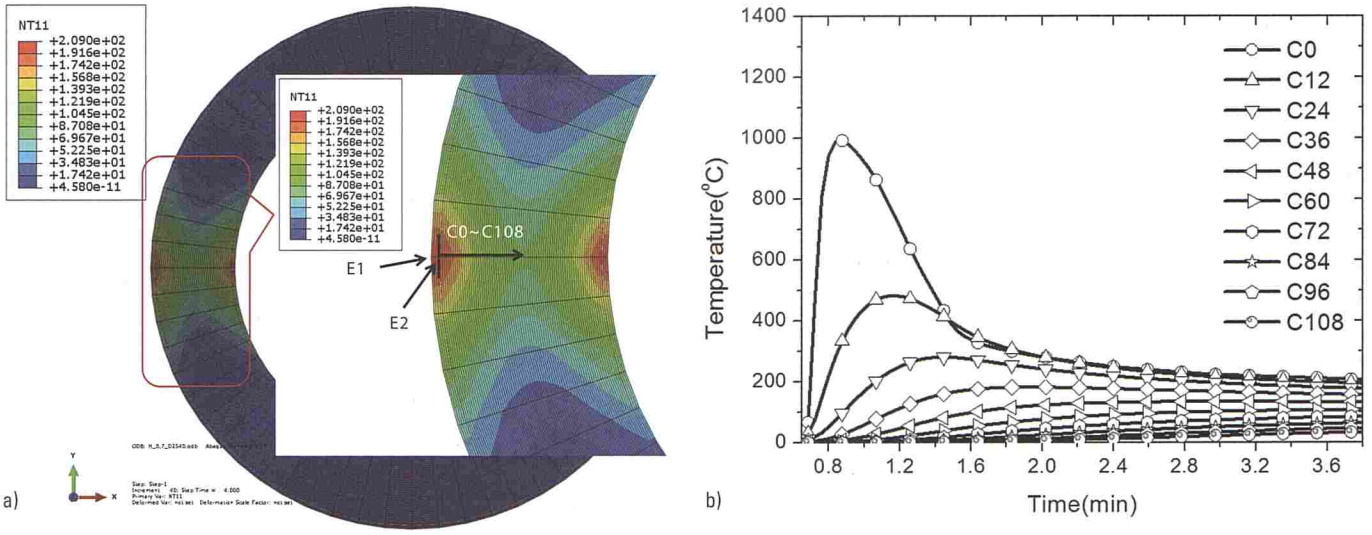

Fig. 5. Temperature distribution due to arc welding: a) temperature distribution on concrete, and b) Time-temperature curves

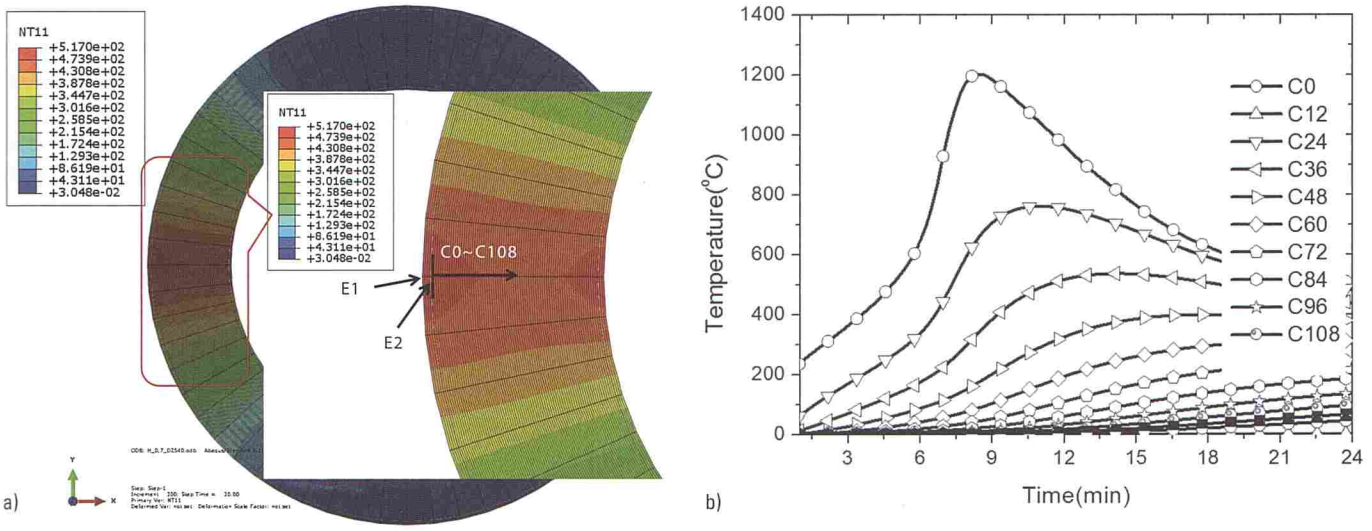

Fig. 6. Temperature distribution due to electro-slag welding: a) temperature distribution on concrete, and b) Time-temperature curves

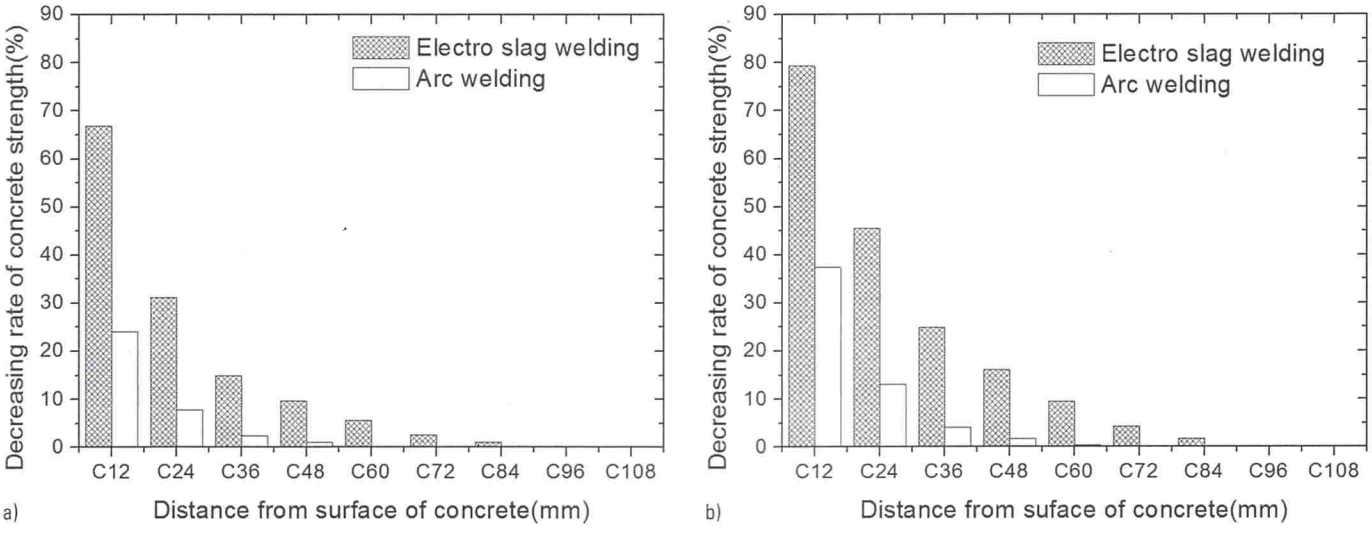

Fig. 7. Comparison of rates of decrease in siliceous concrete strength depending on welding method: a) siliceous, and b) calcareous

(C0–C108) at 12 mm intervals, as shown in Fig. 5a, whereas Fig. 5b shows the Time-temperature curves for arc welding. The tube temperature increases massively because welding heat is applied directly to the tube surface. The temperature increases to max. 200 °C at 12–48 mm from the concrete surface.

Next, the changes in concrete strength due to electro-slag welding heat will be described. An electro-slag welding thermal load was applied to the surface of the internal and external tubes of a precast steel composite hollow column. The temperature distribution and Time-temperature curves for electro-slag welding are shown in Fig. 6.

As shown in Fig. 6a, the temperature at 12 mm from the concrete surface increases to max. 761.95 °C, whereas the temperature at 60 mm from the surface increases to max. 245.17 °C. A comparison with the arc welding case shows that the increase in concrete temperature is considerably greater with electro-slag welding because the latter takes longer and requires a higher welding temperature than arc welding. Therefore, it can be said that electro-slag welding can cause greater damage to concrete than arc welding because the former method uses a greater amount of heat energy. As shown in Figs. 5b and 6b, the temperature distributions of the two welding methods exhibit very different contours. Whereas the high temperatures due to arc welding heat are mainly distributed around the welding heat source, the high temperatures due to electro-slag welding heat are distributed uniformly over the entire section of the precast steel composite hollow column.

Table 2. Hollow ratio and outer diameter of column of analysis models (mm)

Hollow ratio					Outer diameter of column				
D_i/D_o	t_e	t_i	D_o	D_i	D_i/D_o	t_e	t_i	D_o	D_i
0.6	20	15	2540	1470	0.7	20	15	2340	1580
0.7	20	15	2540	1720	0.7	20	15	2540	1720
0.8	20	15	2540	1970	0.7	20	15	2740	1860
0.9	20	15	2540	2220	0.7	20	15	3040	2070

D_i/D_o: hollow ratio, t_e: external tube thickness, t_i: internal tube thickness, D_o: column diameter, D_i: hollow section diameter

Fig. 7 shows the rates of decrease in concrete strength at each location. The rates of strength decrease at 12 mm from the concrete surface are 37.36 and 24.07 % for siliceous and calcareous concretes respectively. As shown in Fig. 7, the rates of strength decrease at 12 mm from the concrete surface are 79.29 and 66.91 % for siliceous and calcareous concretes respectively because of the temperature increase due to electro-slag welding heat. Electro-slag welding induces a more severe strength reduction than arc welding. This implies that the heat conduction of siliceous concrete is more efficient than that of calcareous concrete. The reduction in concrete strength

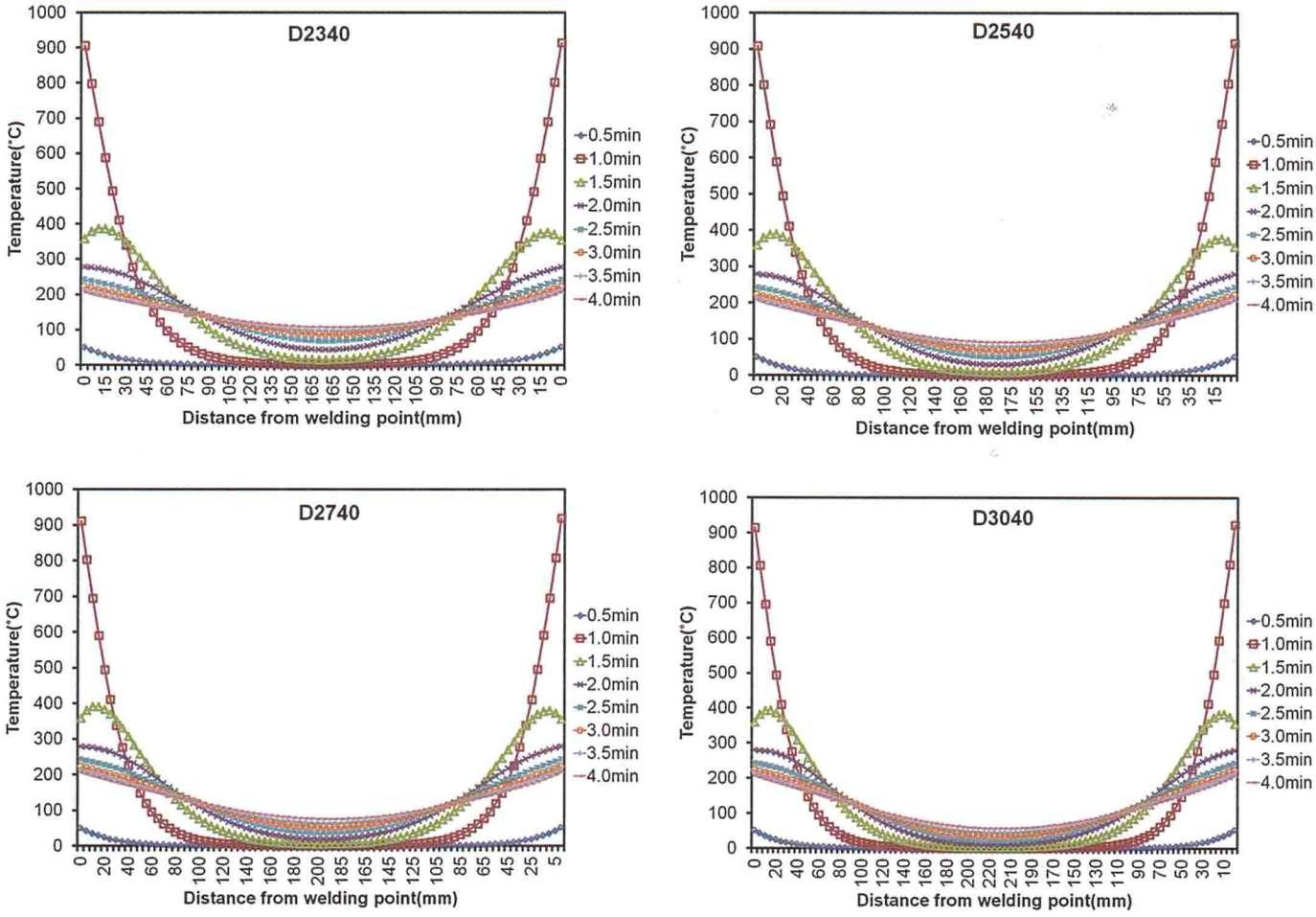

Fig. 8. Temperature change with distance from welding point for arc welding

should be prevented because local damage can extend to global damage.

3.2 Effect of welding heat by diameter and hollow ratio of steel composite hollow column

A steel composite hollow column can be designed with various dimensions considering the direction of applied load and the objective of a particular application. When a steel composite hollow column has to resist large lateral loads with a small axial load on the column, a section with a large diameter and large hollow ratio is essential. By contrast, when a large axial load dominates the structural behaviour, a section with a large diameter and a small hollow ratio is required. The effect of welding heat on the changes in the temperature and strength of steel composite hollow column with different outer diameters and hollow ratios is described below.

Table 2 shows the dimensions of analysis models with the same outer diameter but different hollow ratios, also different outer diameters with same hollow ratio. The hollow ratios are 0.6–0.9, and the diameters of the hollow section are changed depending on the hollow ratio. Furthermore, the outer diameter of the steel composite hollow column was increased from 2340 to 3040 mm in steps of 200 mm, and the diameter of the hollow section was varied under a fixed hollow ratio of 0.7.

Considering the various geometric properties listed in Table 2, a heat transfer analysis is conducted for investigating the changes in concrete strength due to welding heat. The material properties used in this analysis are listed in Table 1, and arc welding and electro-slag welding methods are considered, as shown in Fig. 4.

3.2.1 Effect of arc welding

Firstly, the effects of arc welding heat on the columns with diameters of 2340–3047 mm and a hollow ratio of 0.7 are described. Fig. 8 shows the changes in temperature with distance from the welding point. All models show similar temperature distributions. The concrete around the welding zone shows the highest temperature at 1 min after welding. The analysis result indicates that the concrete of all models sustained the greatest damage during 1–1.5 min after the beginning of arc welding.

Table 3. Temperature and rate of decrease in concrete strength at section midpoint based on diameter of steel composite hollow column for arc welding

Rate of decrease in concrete strength for arc welding			
Diameter	**Temperature (°C)**	**Siliceous**	**Calcareous**
D2340	107.08	2 %	1 %
D2540	90.47	1 %	1 %
D2740	75.37	1 %	1 %
D3040	55.70	0 %	0 %

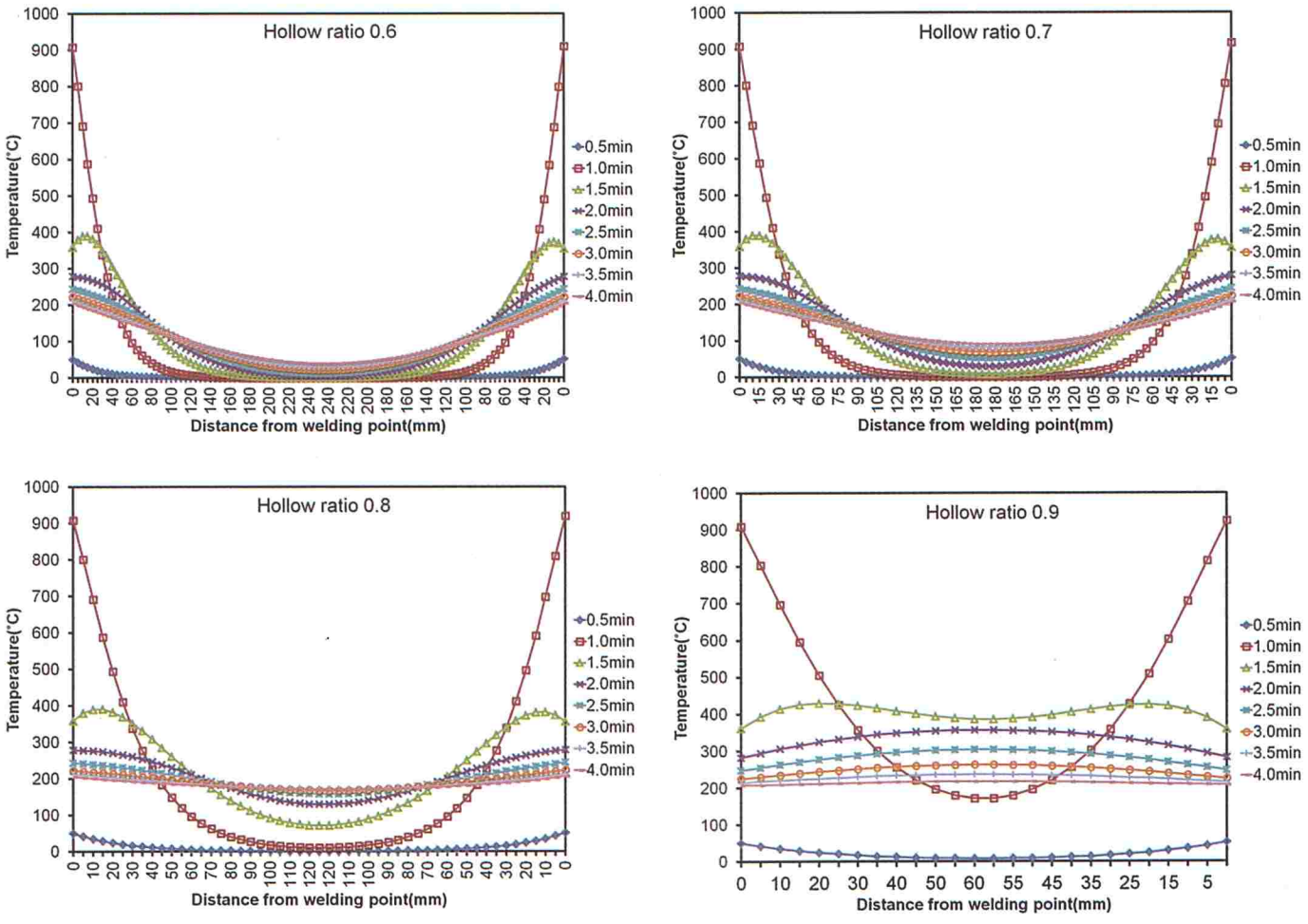

Fig. 9. Temperature change with distance from welding point (hollow ratio 0.6–0.9) for arc welding

The temperature distribution in a steel composite hollow section has a different outer diameter. The temperature at the midpoint of the concrete decreases as the column diameter increases, as can be inferred from Table 3. In this case the midpoint of the concrete of a column with a larger diameter shows relatively less damage. As can be deduced from the table, the rate of decrease in concrete strength is within 2 % for all models considered.

The following paragraphs describe the effect of arc welding heat on columns with the same diameter but different hollow ratios of 0.6–0.9. Fig. 9 shows the change in the temperature based on the distance from the welding point. The concrete temperature due to arc welding is highest at 35 mm from the concrete surface. Fig. 9 shows the change in temperature distribution as the hollow ratio increases. The average concrete temperature rises as the concrete thickness decreases. Whereas steel composite hollow columns with hollow ratios of 0.6–0.7 exhibit a high temperature distribution around the welding zone, the steel composite hollow column with a hollow ratio of 0.9 has the high temperature distribution over the entire section.

Table 4 lists the highest temperature and rate of decrease in concrete strength at the midpoint of a steel composite hollow column. In the case of the model with the hollow ratio of 0.9, the temperature at the section midpoint reaches 389.57 °C, and the strength decrease rates of siliceous and calcareous concrete strength are 23 and 14 % respectively. Thus, when a steel composite hollow column with a hollow ratio of 0.9 is constructed using welding, the effect of arc welding heat on the column should be investigated.

Table 4. Temperature and rate of decrease in concrete strength at section midpoint based on hollow ratio of steel composite hollow column for arc welding

Rate of decrease in concrete strength for arc welding			
Hollow ratio	**Temperature (°C)**	**Siliceous**	**Calcareous**
0.6	38.99	0 %	0 %
0.7	90.47	1 %	1 %
0.8	171.87	4 %	3 %
0.9	389.57	23 %	14 %

3.2.2 Effect of electro-slag welding

The effect of electro-slag welding heat was investigated based on changes in the diameter and hollow ratio of a steel composite hollow column. The material properties listed in Table 1 apply to all models, and the dimensions are subjected to the conditions listed in Table 2. Fig. 10 shows the changes in temperature with distance from the welding point. The temperature at the midpoint of the

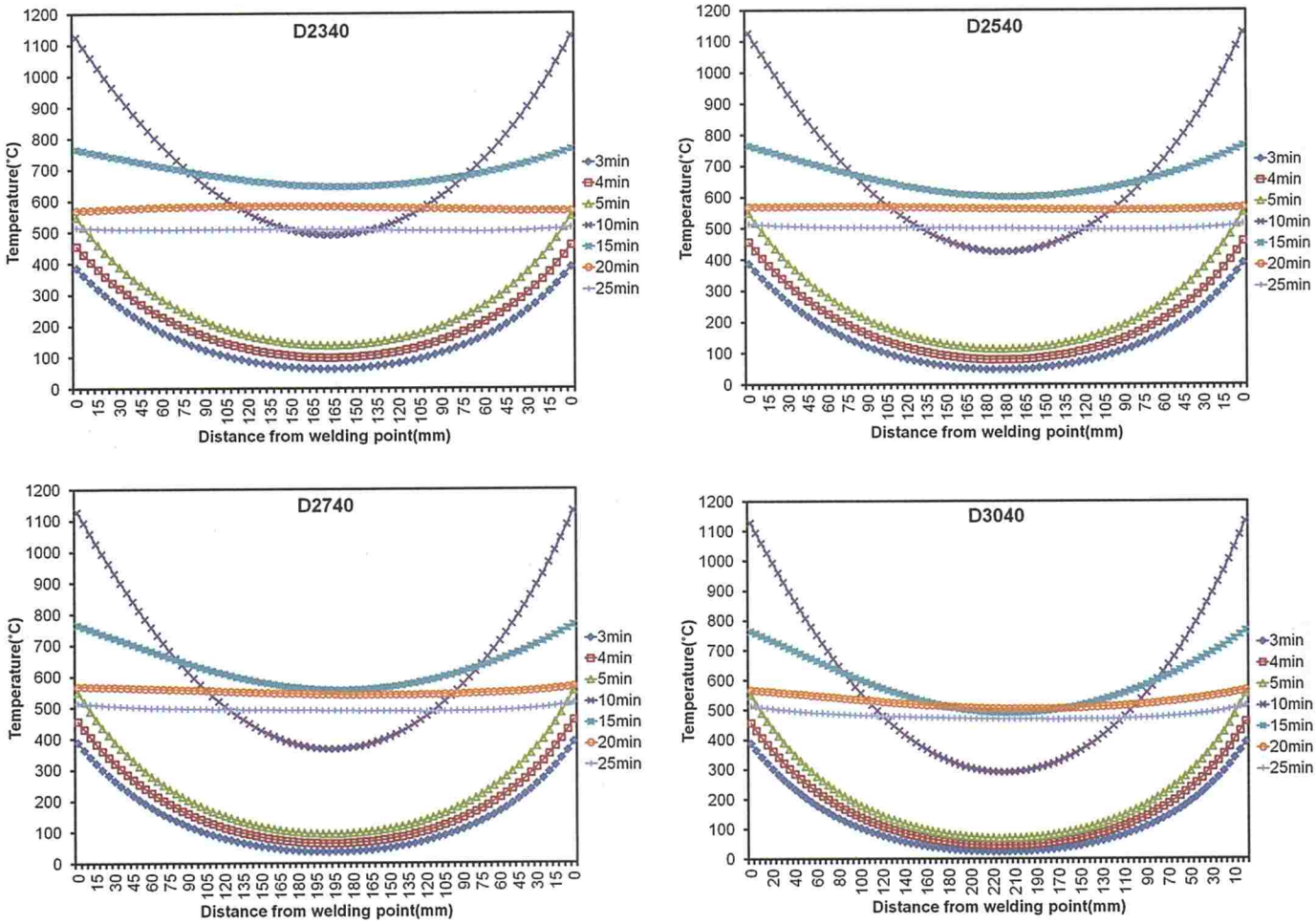

Fig. 10. Temperature change with distance from welding point for electro-slag welding

Table 5. Temperature and rate of decrease in concrete strength at section midpoint based on diameter of steel composite hollow column for electro-slag welding

Rate of decrease in concrete strength for electro-slag welding			
Diameter	**Temperature (°C)**	**siliceous**	**Calcareous**
D2340	646.22	63 %	48 %
D2540	603.61	57 %	41 %
D2740	564.26	50 %	35 %
D3040	510.82	41 %	27 %

Table 6. Temperature and rate of decrease in concrete strength at section midpoint based on hollow ratio of steel composite hollow column for electro-slag welding

Rate of decrease in concrete strength for electro-slag welding			
Hollow ratio	**Temperature (°C)**	**Siliceous**	**Calcareous**
0.6	451.13	32 %	20 %
0.7	603.61	57 %	41 %
0.8	823.53	85 %	76 %
0.9	1111.72	99 %	98 %

steel composite hollow column is < 200 °C, and the temperature around the welding zone is > 400 °C at welding times of 3–5 min. By contrast, the temperature at welding times of 10–25 min is > 500 °C. The temperature at welding times of 15–25 min is constant regardless of the distance from the welding zone. The entire temperature distribution is considerably elevated compared with that for arc welding because electro-slag welding requires longer welding times and results in higher temperatures.

The midpoint temperature decreases with an increase in the tube diameter because the distance from the welding zone increases. The temperature at the midpoint of D2340 is 646.22 °C, and is higher than that of D3040, which is 510.82 °C. The strength decrease rates of siliceous and calcareous concretes are 63 and 48 % respectively for the D2340 column. All models have high temperatures and high concrete strength decrease rates.

For preparing precast steel composite hollow columns according to Table 2 using the electro-slag welding method, hollow ratios are changed from 0.6 to 0.9 in steps of 0.1. Fig. 11 shows the changes in temperature based on the distance from the welding point. The concrete temperature for electro-slag welding shows high change values for 10–25 min. The temperature for the hollow ratio of 0.9 is constant irrespective of the distance from the welding zone for all welding times. The tempera-

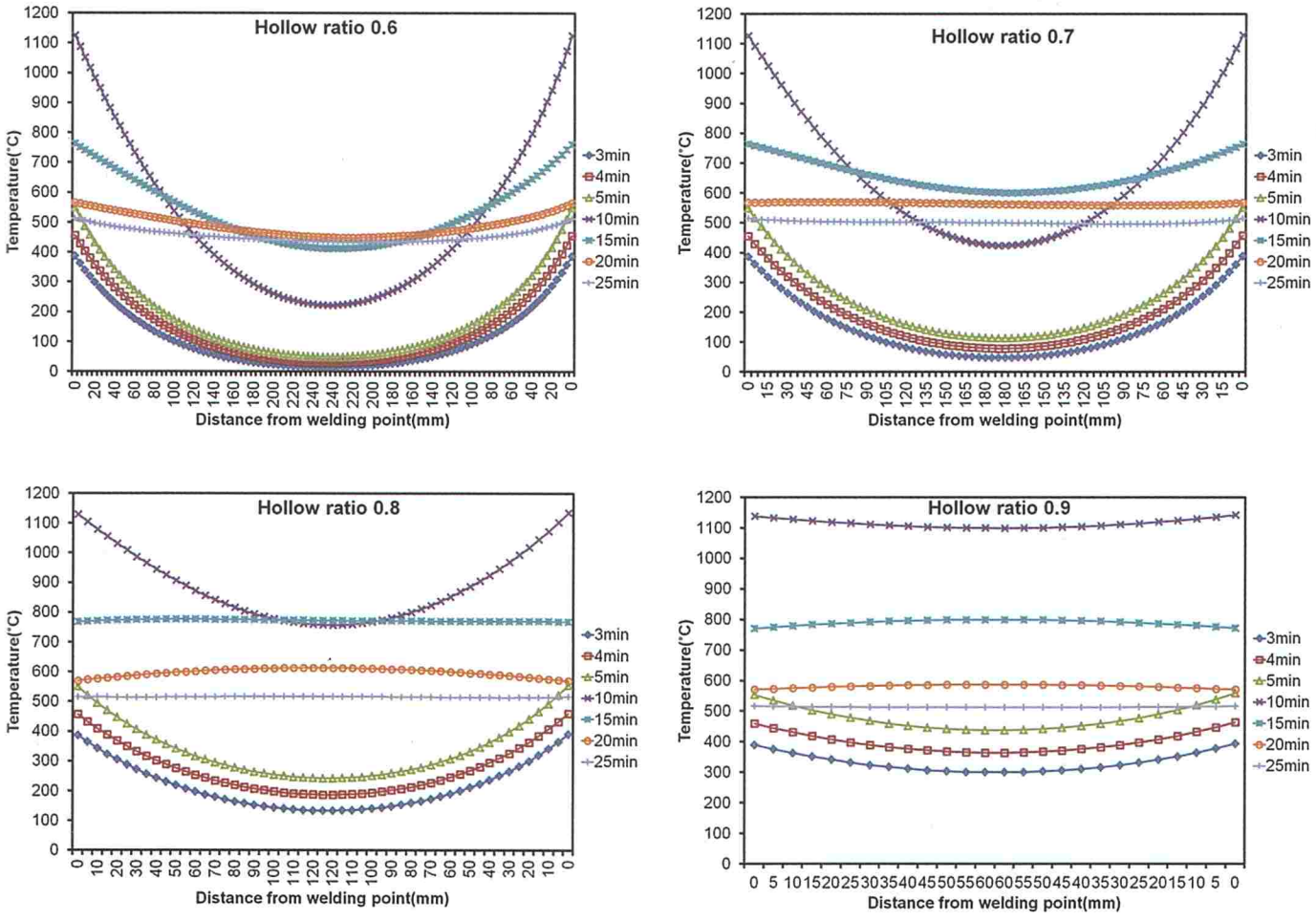

Fig. 11. Temperature change with distance from welding point (hollow ratio 0.6–0.9) for electro-slag welding

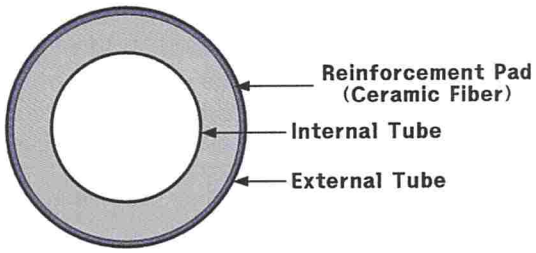

Fig. 12. Ceramic fibre reinforcement

ture is 1100 °C at 10 min. In this case the concrete strength is approximately zero.

As can be inferred from Table 6, the strength decrease ratios of siliceous and calcareous concretes for a hollow ratio of 0.9 are 99 and 98 % respectively. This connection for precast steel composite hollow columns can fail because of damage to the concrete. The solution is to prevent the conduction of welding heat.

Table 7. Dimensions and material properties of ceramic fibres

Property	Value
Continuous service temperature (°C)	1050
Maximum service temperature (°C)	1260
Melting temperature (°C)	1760
Density (kg/m^3)	600
Conductivity (W/m°C)	0.17
Width (mm)	10–150
Thickness (mm)	0.8–10
Length (m)	30/50/100

4 Preventing welding heat conduction

Conduction of welding heat can be blocked or delayed to prevent a drop in concrete strength. Grass or ceramic fibres are very widely used insulators in various construction fields and machines. Glass and ceramic fibres are

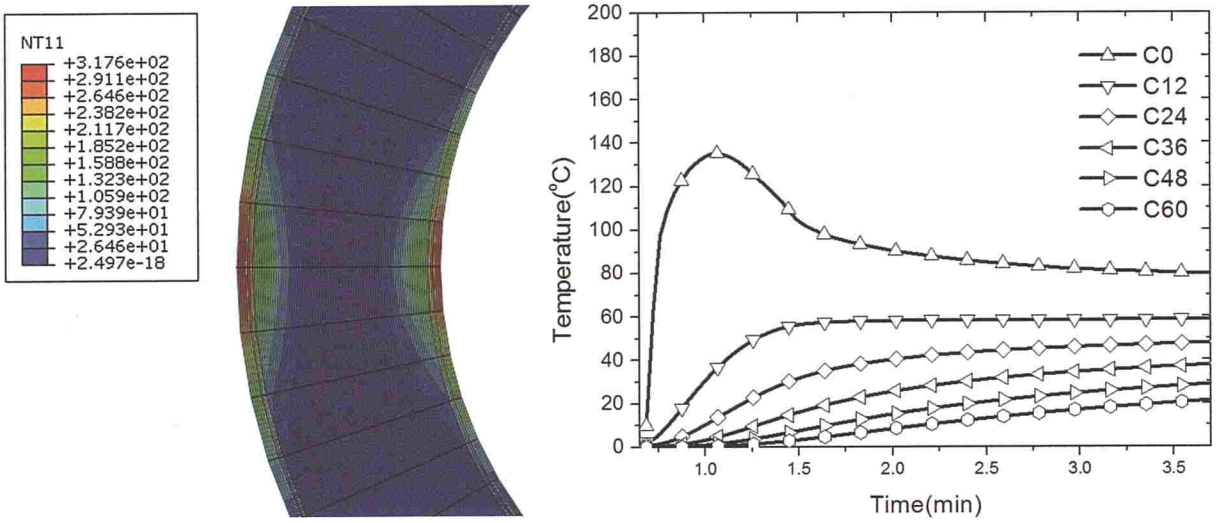

Fig. 13. Temperature distribution with inserted ceramic fibres

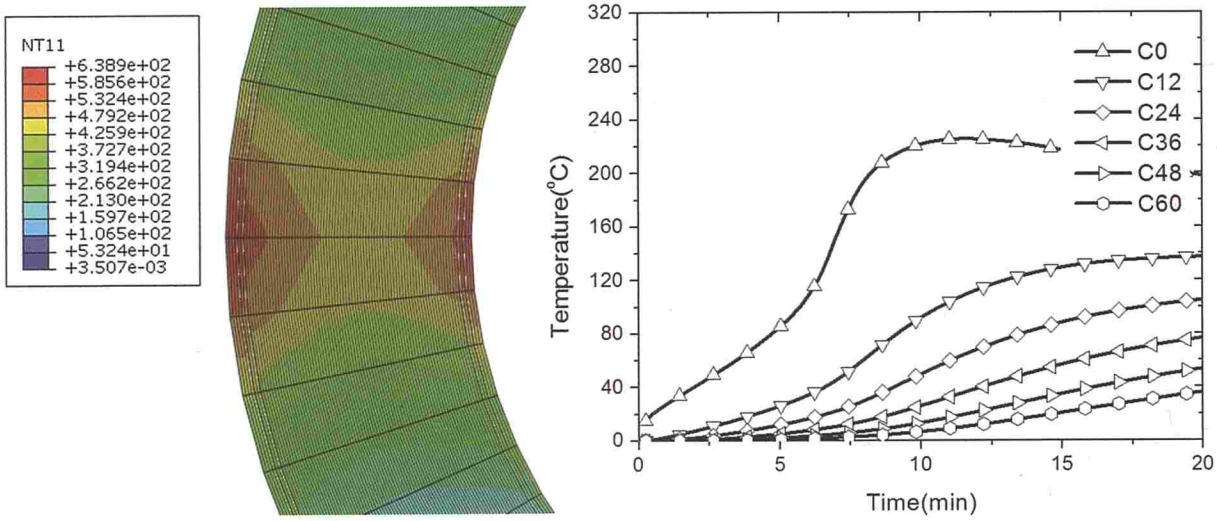

Fig. 14. Temperature distribution after insertion of ceramic fibres

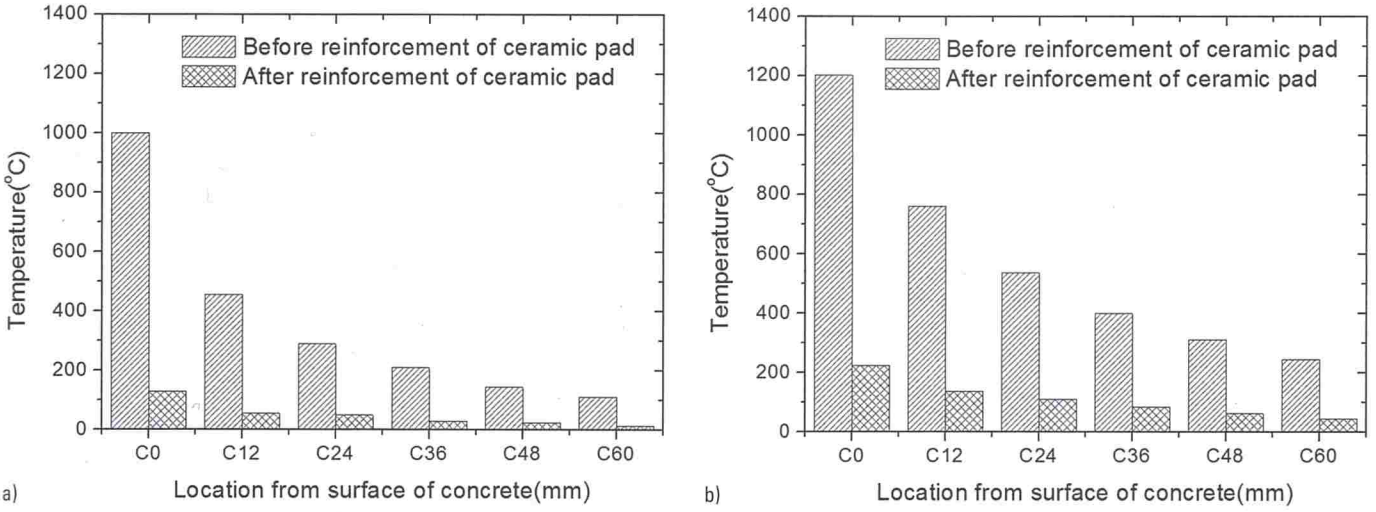

Fig. 15. Temperature before and after adding ceramic reinforcement: a) arc welding, and b) electro-slag welding

very thin and have low density and conductivity values. Inserting ceramic fibres into the space between the concrete and the tubes reduces the conduction of welding heat. Furthermore, the fibres can be partially inserted in the welding zone without having to insert them over the entire area.

When ceramic fibres are inserted into the space between the concrete and the tubes, as shown in Fig. 12, the resulting decrease in heat conduction can be measured through a heat transfer analysis. Table 7 lists the dimensions and material properties of ceramic fibres. These properties were used in the heat transfer analysis. Fig. 13 shows the temperature distribution of a column containing ceramic fibres. The concrete temperature decreases rapidly because the inserted ceramic fibres delay the conduction of welding heat.

Fig. 13 shows the variations in temperature at each location. A temperature of 135.207 °C on the concrete surface after the insertion of ceramic fibres means that the strength decrease rate of the concrete is 2 %. This means that concrete strength barely decreases due to arc welding heat after the insertion of ceramic fibres.

Next, the performance of ceramic fibres is investigated for electro-slag welding. The dimensions and material properties of the ceramic fibres are listed in Table 11.

Fig. 14 shows the temperature distribution for electro-slag welding when ceramic fibres are inserted into the space between the external tube and the concrete. A temperature of 225.61 °C on the concrete surface after the insertion of ceramic fibres means that the strength decrease rate of the concrete is 10 %.

As shown in Fig. 15, the strength decrease rates for concrete drop rapidly depending on the welding method employed. If the thickness of the ceramic fibres is increased, any decrease in concrete strength due to welding can be reduced.

5 Summary and conclusions

This study investigated the effect of the heat generated during the welding of the connections of precast steel composite hollow columns. Two welding methods were studied: arc welding and electro-slag welding. The results of heat transfer analysis led us to draw the following conclusions:

When arc welding was performed on the column, the concrete temperature increased considerably because the welding heat is applied directly to the surface of the tube. The rates of decrease in concrete strength are 37.36 and 24.07 % at 12 mm from the concrete surface for siliceous and calcareous concrete respectively, which affected the adjacent 60 mm. In electro-slag welding, the temperature reached 761.95 °C at 12 mm from the concrete surface. When electro-slag welding was performed, the strength of the concrete decreased by more than that of arc welding. Reinforcement in the form of ceramic fibres inserted in the space between tube and concrete can prevent any decrease in the concrete strength. The temperature of the concrete increased slowly because ceramic fibres delay the conduction of welding heat. If the thickness of the ceramic fibres is increased, the decrease in concrete strength due to welding can be reduced.

Acknowledgments

This research was financially supported by the Korea Institute of Ocean Science & Technology (KIOST), project No. PE99223 & PE99274.

References

1. *Shakir-Khalil, H., Illouli, S.*: Composite columns of concentric steel tubes. Proc. of Conf. on Design and Construction of Non-Conventional Structures, 1987, pp. 73–82.
2. *Wie, S., Mau, S. T., Vipulanandan, C., Mantrala, S. K.*: Performance of new sandwich tube under axial loading: Experiment. Journal of Structural Engineering, 121 (12), 1997, pp. 1806–1814.
3. *Won, D. H., Han, T. H., Kim, S. J., Kang, Y. J.*: Seismic Performance of Fabricated Internally Confined Hollow CFT Column. Korea Society of Civil Engineers 33:2 (2013), pp. 397–407 (in Korean).
4. *Won, D. H., Han, T. H., Lee, D. J., Kang, Y. J.*: A Study of Pier-Segment Joint for Fabricated Internally Confined Hollow CFT Pier. Korea Society of Steel Construction 22:2 (2010), pp. 161–171 (in Korean).

5. Eurocode 2, Design of Concrete Structures – Part 1.2: General rules – Structural Fire Design.
6. *Johannes, B., Sebastian, B. A., Johann, K.*: An innovative design concept for improving the durability of concrete bridges. Structural Concrete 12 2011, pp. 155–163.
7. *Lee, T. K., Chen, C. C., Austin, D. E., Pan, Hsiue, K. Y, Tsai, W. M., Ken, H.*: Experimental evaluation of large circular RC columns under pure compression. Structural Concrete 14, 2013, pp. 60–68.
8. *Park, S. H., Song, K. C., Chung, S. K., Min, B. Y., Choi, S. M.*: An Experimental Study on the Fire Resistance of Concrete-filled Double Skin Tubular Columns. 5th Int. Symp. on Steel Structures, 2009, pp. 299–307.
9. *Zicherman, J.*: Fire Safety in Tall Buildings, McGraw Hill, Inc., 1996.
10. ISO 834: Fire Resistance Tests – Elements of Building Construction, 1999.
11. *Cary, H. B.*: Modern Welding Technology, Prentice Hall, 5th ed., 2002.

Deok Hee Won, PhD
Korea Institute of Ocean Science & Technology
Coastal Development & Ocean Energy Research Division
787 Haeanro, Ansan 426–744
Republic of Korea

Woo Sun Park, PhD
Korea Institute of Ocean Science & Technology
Coastal Development & Ocean Energy Research Division
787 Haeanro, Ansan 426–744
Republic of Korea

Jin-Hak Yi, PhD
Korea Institute of Ocean Science & Technology
Coastal Development & Ocean Energy Research Division
787 Haeanro, Ansan 426–744
Republic of Korea

Sang-Hun Han, PhD
Korea Institute of Ocean Science & Technology
Coastal Development & Ocean Energy Research Division
787 Haeanro, Ansan 426–744
Republic of Korea

Taek Hee Han, PhD (corresponding author)
Korea Institute of Ocean Science & Technology
Coastal Development & Ocean Energy Research Division
787 Haeanro, Ansan 426–744
Republic of Korea